Automated Atlas Fitting for Deep Brain Stimulation Surgery Based on Microelectrode Neuronal Recordings

Eduard Bakštein, Tomáš Sieger, Daniel Novák, Filip Růžička, and Robert Jech

Abstract

Introduction: The deep brain stimulation (DBS) is a treatment technique for late-stage Parkinson's disease (PD), based on chronic electrical stimulation of neural tissue through implanted electrodes. To achieve high level of symptom suppression with low side effects, precise electrode placement is necessary, although difficult due to small size of the target nucleus and various sources of inaccuracy, especially brain shift and electrode bending. To increase accuracy of electrode placement, electrophysiological recording using several parallel microelectrodes (MER) is used intraoperatively in most centers. Location of the target nucleus is identified from manual expert evaluation of characteristic neuronal activity. Existing studies have presented several models to classify individual recordings or trajectories automatically. In this study, we extend this approach by fitting a 3D anatomical atlas to the recorded electrophysiological activity, thus adding topological information. Methods: We developed a probabilistic model of neuronal activity in the vicinity the subthalamic nucleus (STN), based on normalized signal energy. The model is used to find a maximum-likelihood transformation of an anatomical surface-based atlas to the recorded activity. The resulting atlas fit is compared to atlas position estimated from pre-operative MRI scans. Accuracy of STN classification is then evaluated in a leave-one-subject-out scenario using expert MER annotation. Results: In an evaluation on a set of 27 multi-electrode trajectories from 15 PD patients, the proposed method showed higher accuracy in STN-nonSTN classification (88.1%) compared to the reference methods (78.7%) with an even more pronounced advantage in sensitivity (69.0% vs 44.6%). Conclusion: The proposed method allows electrophysiology-based refinement of atlas position of the STN and represents a promising direction in refining accuracy of MER localization in clinical DBS setting, as well as in research of DBS mechanisms.

Keywords

Deep brain stimulation • Anatomical atlas fitting
Microelectrode recordings

1 Introduction

The deep brain stimulation (DBS), targeting the basal ganglia is a symptomatic treatment technique, applied routinely to late-stage Parkinson's disease (PD) and other movement disorders, such as dystonia or essential tremor. In case of the PD, chronic electrical stimulation is most commonly applied to the subthalamic nucleus (STN), which is small (ca 10 mm along its longest axis) and located in subcortical structures, which makes it a challenging target to implant an electrode into. Moreover, brain shift, electrode bending and other influences during the surgery introduce additional inaccuracies into the process.

As highly accurate electrode placement within the nucleus is crucial for achieving a good clinical outcome, most centers use manually evaluated microelectrode recordings (MER) for additional electrophysiological verification of optimal target position. Over more than a decade, successful efforts have been made to provide automatic MER classification to ease the process using various signal-derived features and machine-learning models(e.g. [1, 2]).

In this paper, we extend on the work of Lujan et al. [3], who suggested fitting of a 3D atlas to manually-labeled

E. Bakštein (✉) · T. Sieger · D. Novák
Faculty of Electrical Engineering, Department of Cybernetics, Czech Technical University in Prague, Prague, Czech Republic
e-mail: eduard.bakstein@fel.cvut.cz
URL: http://neuro.felk.cvut.cz/

E. Bakštein
National Institute of Mental Health, Klecany, Czech Republic

T. Sieger · F. Růžička · R. Jech
First Faculty of Medicine, Department of Neurology, Center of Clinical Neuroscience, Charles University, and General University Hospital, Prague, Czech Republic

L. Lhotska et al. (eds.), *World Congress on Medical Physics and Biomedical Engineering 2018*,
IFMBE Proceedings 68/3, https://doi.org/10.1007/978-981-10-9023-3_19

MER locations. Using a probabilistic framework, which we described previously in [4], we develop a model that allows fully automatic fitting of a surface STN atlas directly to raw MER data, without the need for manual annotation.

2 Methods

The proposed model is based on finding a maximum likelihood fit of a surface STN model to neuronal background activity, assuming different probability distribution of neuronal activity level inside and outside the STN. The aim is then to find transformation of the STN atlas, which maximizes the likelihood of STN position with respect to the measured MER data. We use the surface atlas by Krauth et al. [5] but any STN atlas can be used in general. The model is described in more detail below, further technical details can be found in the thesis [6].

To extract an estimate of the neuronal background activity level from raw MER signal, we used the normalized root-mean-square (NRMS) measure proposed in [1], which sets the mean RMS value of the first five recording positions of each trajectory equal to one. This approach compensates for variability in electrode impedance.

2.1 The 3D Atlas Transformation Procedure

We define the 3D transformation used in this study as a matrix operation with 9 degrees of freedom (DOF), allowing translations t_x, t_y and t_z, scaling s_x, s_y and s_z along the x, y and z axis respectively and also rotation around the three axes, given by the angles γ_x, γ_y and γ_z.

The transformation is given by the vector $\boldsymbol{r}$ and can be completely characterized as:

$$\boldsymbol{r} = [t_x, t_y, t_z, s_x, s_y, s_z, \gamma_x, \gamma_y, \gamma_z]. \quad (1)$$

2.2 Model Structure

The model assumes two states with different NRMS levels: (i) Inside the STN (*IN*) and (ii) outside the STN (*OUT*). The probability distribution of the NRMS values in each state is modeled by the log-normal distribution in what we call the *emission probabilities*. Additionally, we incorporate smooth transition between states around the boundary, modeled by logistic (sigmoid) function, which we call the *sigmoid membership function*. This provides smooth gradient for more convenient optimization, as well as a more realistic representation of the electrophysiological boundary of the STN, which is fuzzy especially at the lateral end (see Fig. 2). The emission probabilities, as well as parameters of the sigmoid membership functions are estimated during model *training phase* on data from the training set and form the parameter vector $\boldsymbol{\Theta}$.

The atlas fitting is then done during the *evaluation phase*, typically on unseen test data. The aim is to find a transformation vector $\boldsymbol{r}^*$ which maximizes the likelihood of producing a set of observations (i.e. NRMS values) $\boldsymbol{x} = \{x_1, \ldots, x_N\}$ recorded at locations $\boldsymbol{L} = \{\boldsymbol{l}_1, \ldots, \boldsymbol{l}_N\}$, where $\boldsymbol{l_i}$ are the 3D recording site coordinates corresponding to observation x_i. The transformation using the parameters $\boldsymbol{r}$ is then applied to the STN atlas vertices $\boldsymbol{v}$ at the initial position. All parameters from the vector $\boldsymbol{\Theta}$ are held fixed during the whole evaluation phase.

Emission probabilities The emission probabilities represent how likely a background activity (NRMS) level x_i is to be observed in the respective state. The emission probabilities are modeled using the log-normal distribution, whose parameters $\{\hat{\mu}_{OUT}, \hat{\sigma}_{OUT}, \hat{\mu}_{IN}, \hat{\sigma}_{IN}\}$ are estimated during the training phase using standard maximum-likelihood estimation. Example of trained emission probabilities can be found in Fig. 1.

In the evaluation phase, the emission probability $p(x_i|s, \boldsymbol{\Theta})$ of observing NRMS value x_i in a state s given model parameters $\boldsymbol{\Theta}$ is calculated using formula for probability density function of the log-normal distribution.

Membership probabilities The transition between states is modeled by the membership sigmoid function S, which also represents the fuzzy electrophysiological boundary of the STN, as observed on real data (see Fig. 2). As the slope of the transition is steeper at the proximal boundary (where the electrode enters the STN) the training NRMS data aligned with respect to the STN entry, combined with mirrored data aligned with respect to the STN exit are used to fit a single sigmoid function S, defined by two parameters: shift β_0 and slope β_1.

In the *evaluation phase*, the sigmoid transition function depends only on the distance from the model surface, rotated using vector $\boldsymbol{r}$ and is computed according to:

$$S(\boldsymbol{d_i}|\boldsymbol{\Theta}) = \left(1 + \exp -(\beta^0 + \beta^1(d_i))\right)^{-1}, \quad (2)$$

where d_i is the euclidean distance between the MER measurement location $\boldsymbol{l_i}$ and the nearest point on the surface of the STN model. Additionally, the distance d_i is multiplied by -1 if the location $\boldsymbol{l_i}$ lies outside of the model and by $+1$ when inside.

The membership probabilities for trained model parameters $\boldsymbol{\Theta}$ and anatomical model transformed by the vector $\boldsymbol{r}$ are then computed according to:

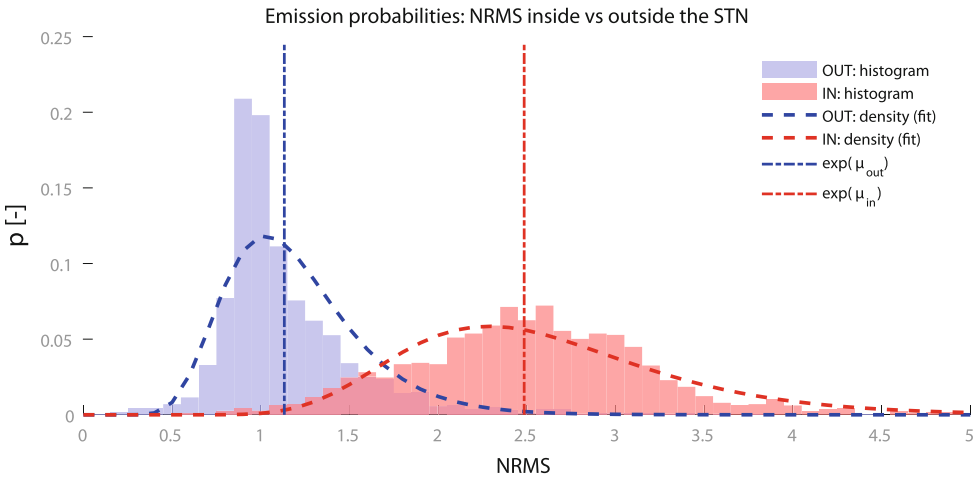

Fig. 1 Fitted emission probabilities: histograms of observed NRMS values inside (red area) and outside (blue area) the STN, with fitted log-normal probability density functions (dashed curves) and their parameters (vertical lines) (Color figure online)

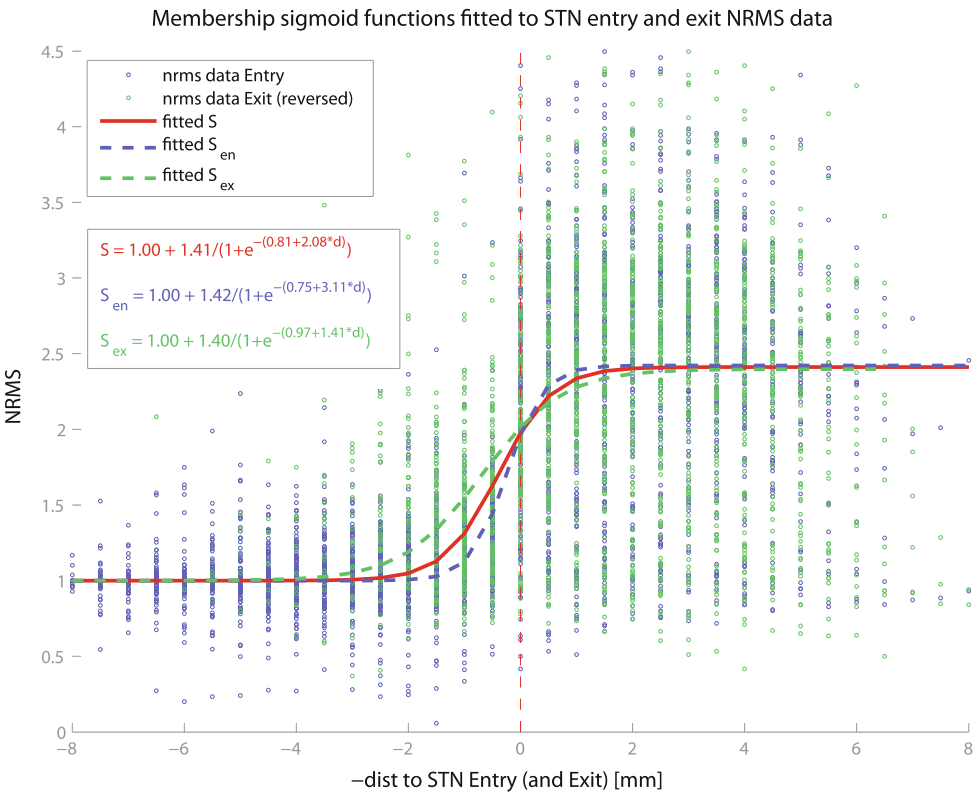

Fig. 2 The membership logistic sigmoid function S (red) fitted to measured NRMS data around the STN entry (blue circles) and exit (green circles, depth-flipped/negative) data. The fitted sigmoid S can be compared to separate entry and exit sigmoid S_{en} and S_{ex}, fitted on STN entry or exit data separately (Color figure online)

$$p(\boldsymbol{l_i} \in IN|\boldsymbol{r}, \boldsymbol{\Theta}) = S(l_i|\boldsymbol{r}, \boldsymbol{\Theta}) \tag{3}$$

for the state IN and:

$$p(\boldsymbol{l_i} \in OUT|\boldsymbol{r}, \boldsymbol{\Theta}) = 1 - p(\boldsymbol{l_i} \in IN|\boldsymbol{r}, \boldsymbol{\Theta}) \tag{4}$$

for the state OUT.

The trained model is fully characterized by the parameter vector.

$\boldsymbol{\Theta} = \{\hat{\mu}_{OUT}, \hat{\sigma}_{OUT}, \hat{\mu}_{IN}, \hat{\sigma}_{IN}, \beta^0, \beta^1\}$, comprising parameters of the emission probability densities and those of the sigmoid function.

Likelihood function and MLE estimation The aim of optimization in the evaluation phase is to find transformation vector $\boldsymbol{r}^*$, which maximizes the likelihood given the observed data:

$$\boldsymbol{r}^* = \underset{\boldsymbol{r}}{\text{arg max}}\, \mathcal{L}(\boldsymbol{r}|\{\boldsymbol{x}, \boldsymbol{L}\}, \boldsymbol{\Theta}) = \underset{\boldsymbol{r}}{\text{arg max}}\, p(\{\boldsymbol{x}, \boldsymbol{L}\}|\boldsymbol{r}, \boldsymbol{\Theta}) \tag{5}$$

Where p is the joint probability of observation sequence $\boldsymbol{x}$ at locations $\boldsymbol{L}$, given trained model parameters $\boldsymbol{\Theta}$ and transformation vector $\boldsymbol{r}$. When decomposed, the probability of being in state s (i.e. IN or OUT) and observing a NRMS value x_i at position $\boldsymbol{l_i}$ is computed as a product of the

emission and membership probability functions according to the Bayes' theorem:

$$p(\{x_i, \boldsymbol{l_i} \in \boldsymbol{s}\}|\boldsymbol{r}, \boldsymbol{\Theta}) = p(x_i|\boldsymbol{l_i} \in \boldsymbol{s}, \boldsymbol{r}, \boldsymbol{\Theta}) \cdot p(\boldsymbol{l_i} \in \boldsymbol{s}|\boldsymbol{r}, \boldsymbol{\Theta}) \quad (6)$$

The joint probability for a single observation is then computed as a marginalization over both states:

$$\begin{aligned} p(\{x_i, \boldsymbol{l_i}\}|\boldsymbol{r}, \boldsymbol{\Theta}) &= p(\{x_i, \boldsymbol{l_i}\}|\boldsymbol{r}, \boldsymbol{\Theta}) = \\ &= p(\{x_i, \boldsymbol{l_i} \in IN\}|\boldsymbol{r}, \boldsymbol{\Theta}) \\ &\quad + p(\{x_i, \boldsymbol{l_i} \in OUT\}|\boldsymbol{r}, \boldsymbol{\Theta}) \end{aligned} \quad (7)$$

To compute the joint probability of the whole observation sequence $\boldsymbol{x} = \{x_1, \ldots, x_N\}, \boldsymbol{L} = \{\boldsymbol{l_1}, \ldots, \boldsymbol{l_N}\}$, we naïvely assume conditional independence given model parameters and compute the joint probability as:

$$p(\{\boldsymbol{x}, \boldsymbol{L}\}|\boldsymbol{r}, \boldsymbol{\Theta}) = \prod_{i=1}^{N} p(\{x_i, \boldsymbol{l_i}\}|\boldsymbol{r}, \boldsymbol{\Theta}) \quad (8)$$

For numerical stability, we use the equivalent task and minimize the negative log-likelihood instead:

$$\boldsymbol{r}^* = \underset{\boldsymbol{r}}{arg\min} \sum_{i=1}^{N} -\ln(p(\{x_i, \boldsymbol{l_i}\}|\boldsymbol{r}, \boldsymbol{\Theta})), \quad (9)$$

where $\boldsymbol{r}^*$ is the MLE estimate of optimal transformation parameters, given the model parameters and the observation sequence. The minimization is performed using general purpose constrained optimization (the *active set* algorithm as implemented in MathWorks Matlab `fmincon` function). To prevent the model from diverging from clinically reasonable scaling and rotation, we set the maximum shift to ± 5 mm in any direction, maximum scaling $\pm 25\%$ in each direction and rotation maximum $\pm 15^\circ$ around each axis, hence the model abbreviation *nrmsCon*, used below.

2.3 Reference Methods

In order to evaluate performance of the proposed method, we implemented three reference methods, based solely on anatomical landmarks, identified manually by neurologists in the pre-operative MRI images:

1. **target**—the method consists in finding a translation $[t_x, t_y, t_z]$, which shifts central point of the atlas model to the planned target point without any scaling or rotation. This method is also used as the initalization for NRMS-based fitting, as it requires no additional information apart from planned target coordinates, which is the result of standard pre-surgical planning procedure.
2. **acpc**—this method represents a simple atlas fitting approach, based on two significant brain landmarks: the anterior commisure (AC) and the posterior commisure (PC). The method analytically finds a full 9-DOF transformation which maps the vector given by AC and PC points in the atlas to the vector given by AC-PC points, identified in patient's MRI scans.
3. **allpoints**—additionally to the AC-PC points, this method uses 12 landmarks on the STN boundaries, defined previously in the supplement of [7]. The method than finds a full 9-DOF transformation to minimize the least-square distance between the characteristic points on the atlas and in manually annotated patient MRI data.

2.4 Data Collection and Preprocessing

The MER signals were recorded intra-operatively from five parallel electrode trajectories, spaced 2 mm apart in a "ben-gun" configuration around the central electrode. The sampling frequency was 24 kHz, signals were filtered by a bandpass filter in the range 500–5000 Hz upon recording and stored for offline processing. At each of the recording positions, spaced apart by 0.5 mm, a typically ten seconds of MER signal were recorded using each electrode. In order to eliminate artifact-bearing segments of the signals, we used our automatic artifact classifier, presented previously in [8]. Manual intra-operative expert annotation of the MER signals has been stored, labeling each signal as coming either from inside or outside the STN.

2.5 Performance Evaluation

In order to estimate the out of sample performance of the proposed method and due to the relatively small sample size (in terms of whole patient sets), we employed the leave one subject out (LOSO) procedure. In each iteration we kept one subject's data (maximum two 5-electrode trajectories for bi-laterally implanted patients) for model fitting and evaluation, while all other data were used to obtain the parameters $\boldsymbol{\Theta}$.

To evaluate quality of the model fit, we used the machine-learning based approach used also in [3]: the MER recording sites, expert-labeled as STN, were expected to be encapsulated inside the fitted atlas (true positives), while other recordings were expected to lie outside. The accuracy, sensitivity, specificity and Youden J-index ($J = sensitivity + specificity - 1$) were computed.

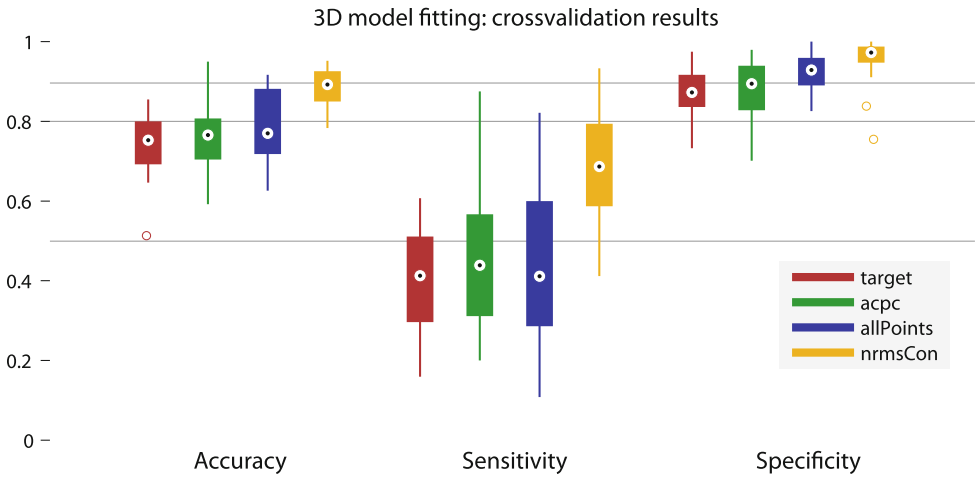

Fig. 3 Comparison of classification performance across methods (correctly included/excluded recorded NRMS points): the proposed electrophysiology-based method *nrmsCon* (yellow) showed higher STN identification accuracy than the reference MRI-based methods (Color figure online)

Table 1 Overall 3D STN model fitting crossvalidation results on the 27 validation trajectories for all methods

Method	Accuracy		Sensitivity		Specificity		Youden J	
	Mean (%)	Std (%)	Mean (%)	Std	Mean (%)	Std	Mean (%)	Std (%)
Target	**74,3**	7,6	**40,7**	12,3	**87,3**	5,7	**28,0**	17,0
acpc	**75,7**	8,9	**44,7**	17,2	**87,6**	8,2	**32,3**	21,1
All Points	**78,7**	8,7	**44,6**	19,8	**92,3**	4,9	**36,8**	21,3
nrmsCon	**88,1**	5,2	**69,0**	14,2	**95,5**	5,4	**64,5**	13,6

3 Results and Discussion

3.1 Collected Data

The dataset contained data from 27 explorations in 15 PD patients with complete 3D information and additional 8 explorations from 4 patients with measured and annotated MER signals but without information on spatial recording locations. The latter small set was included for estimation of model parameters ($\boldsymbol{\Theta}$) but was excluded from validation. Each exploration consisted of 5 electrode trajectories with 25.9 recording positions on average. In total, the data included 35 explorations from 19 patients, leading to 175 electrode trajectories and 4538 recorded MER signals.

3.2 Performance Evaluation

Classification performance (i.e. the proportion of correctly included/excluded recording sites) was evaluated for each of the fitting methods on the 27 exploration trajectories, the results are shown in the Fig. 3 and Table 1. As seen from the results, it is apparent that the presented *nrmsCon* method provided substantially better fit to the measured MER sites than any of the other methods. The results further show, that the main difference is driven especially by the higher sensitivity, i.e. the proportion of correctly included STN points inside the model. This is even more clearly seen from the tabulated values of the Youden J statistic, where the proposed method surpasses the reference methods by a factor of two. It has to be considered that the dataset is highly imbalanced dataset with only 27% of signals coming from the STN.

To provide additional insight into the results, we evaluated the fitted values of the transformation parameters individually. Results of the proposed *nrmsCon* method showed similar distribution to the landmark-based *allPoints* method, except for a relatively large ca 2 mm shift in the y direction. According to previous studies [9], this is the main direction of the brain shift occuring during surgery and this preliminary evaluation thus provides promising results for intra-operative brain-shift compensation. An example visualization of atlas fit can be found in Fig. 4.

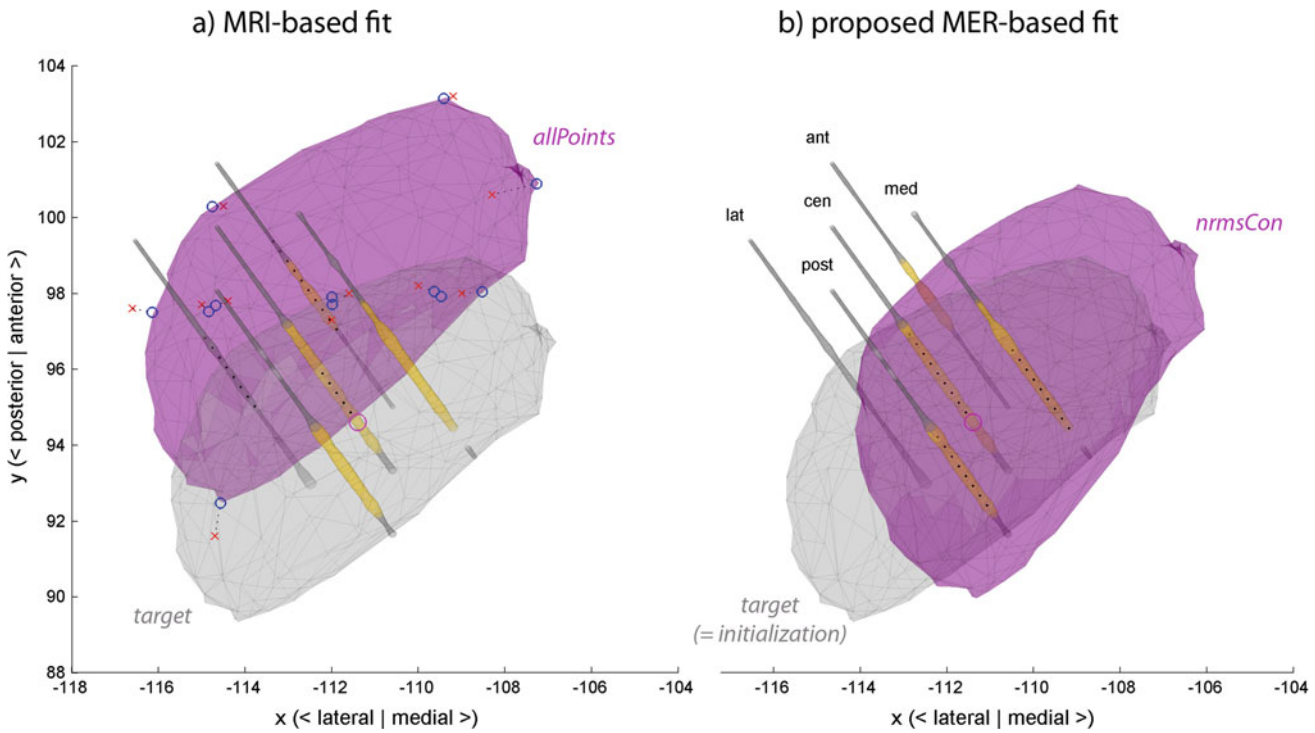

Fig. 4 Examples of model fit using the **a** *allPoints* method based on characteristic MRI points in patient pre-operative scans (red x) and on the atlas (blue o) and **b** the proposed *nrmsCon* method based solely on electrophysiology on a single five-electrode trajectory. The final model position after fitting is shown in purple, the initial position (*target* method) is shown in grey. The width of the five microelectrode trajectory cyllinders denotes the NRMS value, while colors denote manual labels: STN in yellow, non-STN in grey. MER positions inside the resulting model are denoted by black points, planned target by red o (Color figure online)

4 Conclusion

We proposed a probabilistic model for automatic direct fitting of a STN atlas to multi-electrode explorative DBS MER data. The presented results indicate that the proposed MER-based system may potentially bring increased accuracy in intra-operative MER localization and thus contribute to higher efficacy in DBS research and potentially also in therapy.

Acknowledgements The work presented in this paper was supported by the Czech Science Foundation (GACR), under grant no. 16-13323S and by the Ministry of Education Youth and Sports, under NPU I program Nr. LO1611.

References

1. Anan Moran, Izhar Bar-Gad, Hagai Bergman, and Zvi Israel. Real-time refinement of subthalamic nucleus targeting using Bayesian decision-making on the root mean square measure. *Mov Disord*, 21(9):1425–1431, September 2006.
2. Adam Zaidel, Alexander Spivak, Lavi Shpigelman, Hagai Bergman, and Zvi Israel. Delimiting subterritories of the human subthalamic nucleus by means of microelectrode recordings and a Hidden Markov Model. *Mov Disord*, 24(12):1785–1793, sep 2009.
3. J. Luis Lujan, Angela M. Noecker, Christopher R. Butson, Scott E. Cooper, Benjamin L. Walter, Jerrold L. Vitek, and Cameron C. McIntyre. Automated 3-Dimensional Brain Atlas Fitting to Microelectrode Recordings from Deep Brain Stimulation Surgeries. *Stereotactic and Functional Neurosurgery*, 87(4):229–240, jan 2009.
4. Eduard Bakstein, Tomas Sieger, Daniel Novak, and Robert Jech. Probabilistic Model of Neuronal Background Activity in Deep Brain Stimulation Trajectories. In *Information Technology in Bio- and Medical Informatics - 7th International Conference, (ITBAM)*, 2016.
5. Axel Krauth, Remi Blanc, Alejandra Poveda, Daniel Jeanmonod, Anne Morel, and Gabor Szekely. A mean three-dimensional atlas of the human thalamus: Generation from multiple histological data. *NeuroImage*, 49(3):2053–2062, 2010.
6. Eduard Bakstein. *Deep Brain Recordings in Parkinson's Disease: Processing, Analysis and Fusion with Anatomical Models*. doctoral thesis, Czech Technical University in Prague, 2016.
7. Tomas Sieger, Tereza Serranova, Filip Ruzicka, Pavel Vostatek, Jiri Wild, Daniela Stastna, Cecilia Bonnet, Daniel Novak, Evzen Ruzicka, Dusan Urgosik, and Robert Jech. Distinct populations of neurons respond to emotional valence and arousal in the human subthalamic nucleus. *Proceedings of the National Academy of Sciences of the United States of America*, 112(10):3116–21, 2015.

8. Eduard Bakstein, Tomas Sieger, Jiri Wild, Daniel Novak, Jakub Schneider, Pavel Vostatek, Dusan Urgosik, and Robert Jech. Methods for automatic detection of artifacts in microelectrode recordings. *Journal of Neuroscience Methods*, 290:39–51, 2017.

9. Srivatsan Pallavaram, Benoit M. Dawant, Michael S. Remple, Joseph S. Neimat, Chris Kao, Peter E. Konrad, and P. F. D'Haese. Effect of brain shift on the creation of functional atlases for deep brain stimulation surgery. *International Journal of Computer Assisted Radiology and Surgery*, 5(3):221–228, 2010.